Spatial heterogeneity of soil properties in relation to microtopography in a non-tidal rewetted coastal mire

S. Ahmad[1], H. Liu[1], F. Beyer[2], B. Kløve[3], B. Lennartz[1]

[1]Soil Physics, Faculty of Agriculture and Environmental Sciences, University of Rostock, Germany
[2]Geodesy and Geoinformatics, Faculty of Agriculture and Environmental Sciences, University of Rostock, Germany
[3]Water, Energy and Environmental Engineering Research Unit, University of Oulu, Finland

SUMMARY

Over the past century, mires and peatlands have faced a wide range of degradation by artificial drainage, making them one of the most threatened ecosystems in Europe. However, restoration of drained peatlands has gained much importance over the last three decades, mostly due to the multiple ecosystem services they provide such as carbon storage, habitat provision and water flow regulation. Although there has been an increased focus on such ecosystems, spatial research on hydrophysical soil properties following rewetting in coastal mires is lacking. Therefore, the objectives of the study were to understand the spatial structures of hydrophysical properties of organic soils and spatial patterns of organic matter accumulation in relation to soil surface microtopography. Soil organic matter content (SOM) and hydraulic conductivity (K_s) of topsoils (0–28 cm), along with soil textures of the underlying mineral substrate, were investigated in a rewetted non-tidal coastal flood mire (Baltic Sea). The results indicate that the organic horizon with its relatively low K_s acts as a hydrological barrier to infiltration. Soil organic matter content (SOM), K_s and soil surface microtopography are all spatially auto-correlated within 100, 87 and 53 m, respectively. Bivariate Moran's I revealed a positive but weak spatial correlation between SOM and K_s and a moderately strong negative spatial correlation between SOM and soil surface microtopography. A map of SOM was generated using simple kriging, which predicts higher SOM in the centre of the ecosystem, at lower elevations; and lower SOM at the edges of the study area, at higher elevations. Local depressions in the centre of the ecosystem provide a wetter and therefore more anaerobic environment, thereby decreasing carbon mineralisation rates and enabling peat accumulation. The low hydraulic conductivity of the degraded peat in the presence of lower micro-elevations in the centre of the ecosystem is likely to increase the residence time of floodwater and thus may enhance (new) peat accumulation. Thus, we conclude that, for the restoration of non-tidal coastal mires where flooding events are not as frequent, K_s and soil surface microtopography are even more important factors to consider than for tidal systems.

KEY WORDS: hydraulic conductivity, peatland, restoration, soil organic matter, spatial variability

INTRODUCTION

Mires and peatlands account for only 3 % of the global land surface (Yu *et al.* 2010), primarily occurring in boreal and temperate regions, with a smaller proportion in the tropics. Nevertheless, they may store of up to 644 Gt of carbon (Yu *et al.* 2010, Page *et al.* 2011, Dargie *et al.* 2017) or about 21 % of the global total soil organic carbon stock of 3000 Gt (Scharlemann *et al.* 2014, Leifeld & Menichetti 2018). Carbon sequestration and greenhouse gas emissions avoidance through peatland restoration have been recognised as climate change mitigation strategies. Furthermore, at present, human activities are either draining or mining about 12 % of global peatlands (Joosten 2010), thereby changing them from long-term carbons sinks into sources (Leifeld & Menichetti 2018) by accelerating the carbon mineralisation process of soil organic matter (Brandyk *et al.* 2002).

Mires and peatlands that are located in low-lying coastal areas are of particular interest, as coastal wetlands sustain the highest rates of carbon sequestration per unit area of all ecosystems (Rogers *et al.* 2019). In low-lying coastal areas, peatlands form by the accumulation of organic material over millennia and are often regarded as the interface between the land and the sea. While there is a large uncertainty in terms of the total land area of coastal peatlands (Henman & Poulter 2008), analysis by Chmura *et al.* (2003) reveal that saline wetland soils (including salt marshes and mangrove swamps)

store more than 10,000 Tg of carbon. Nevertheless, coastal peatlands face additional threats from climate change as rising global sea levels may drive future releases of stored carbon (Henman & Poulter 2008, Whittle & Gallego-Sala 2016).

Drainage of peatlands can alter hydro-physical properties of peat soils such as soil organic matter content (Heller & Zeitz 2012), pore structure and hydraulic conductivity (Zeitz & Velty 2002, Liu *et al.* 2016, Rezanezhad *et al.* 2016) and consequently may alter hydrological processes (Holden & Burt 2003, Holden *et al.* 2006) as well as change water chemistry (Holden *et al.* 2004) and vegetation composition (Schrautzer *et al.* 2013). As hydraulic properties control soil moisture, they in turn drive carbon and nitrogen dynamics (Kluge *et al.* 2008). For example, under water-saturated conditions, the low oxygen available limits microbial activity and CO_2 fluxes (Säurich *et al.* 2019). Denitrification is limited by water availability while nitrification is limited by aeration (Säurich *et al.* 2019). Thus, when there is a lack of soil moisture, aeration of the peat and subsequent mineralisation and nitrification of organic nitrogen releases large amounts of nitrates (Holden *et al.* 2004, Tiemeyer & Kahle 2014).

Soil surface microtopography, which is the micro-elevation of the surface of the soil (Li & Chen 2012), can have a large influence on flow processes at the soil surface (Fox *et al.* 1998, van der Ploeg *et al.* 2012). Microtopographic variation translates into differences in hydrology within a wetland, with topsoil and vegetation being drier at higher elevations than in depressions because of increased distance from the water table (Benscoter *et al.* 2005). Therefore, microtopography can give a good insight into the wetness of a given area, influenced by both groundwater and surface water dynamics, and thus can be associated with spatial patterns in soil organic matter content (SOM). For example, Zheng *et al.* (2019) showed that there is less SOM at higher elevations because it decomposes faster under aerobic conditions than under anaerobic conditions.

Soil organic matter content and bulk density are generally negatively correlated both in mineral soils (Adams 1973, Rawls 2004, Perie & Ouimet 2008, Liu & Lennartz 2019a) and in organic soils (Adams 1973, Perie & Ouimet 2008, Liu & Lennartz 2019a). Additionally, SOM and total porosity are positively correlated (Kechavarzi *et al.* 2010, Grover & Baldock 2013, Liu & Lennartz 2019a). Furthermore, SOM and K_s have been found to be positively correlated according to Zare *et al.* (2010), Nath & Krishna (2014) and Zhang *et al.* (2018) for mineral soils and by Boelter (1969) and Liu & Lennartz (2019a) for peat soils.

Although it is well acknowledged that physical soil properties and hydraulic parameters have spatial dependencies (Bevington *et al.* 2016), our understanding of spatial variability of hydrophysical properties of organic soils is limited compared to that of mineral soils (Lewis *et al.* 2012). There is a wealth of studies which predict mineral soil properties as part of the digital soil mapping literature (Ma *et al.* 2019), some of which focus on peat (Minasny *et al.* 2019), although most of these studies focus on much larger scales (e.g. subnational, national, regional, global) than that of the present study. Digital mapping methodology combines field observations with factors that are known to affect soil properties. For example, Rudiyanto *et al.* (2018) utilised digital elevation models, geographical information and radar images, along with machine learning models, to derive spatial prediction functions and map peat thickness on an island in Indonesia. Kriging methods have also been used in several studies to predict peat thickness (Beilman *et al.* 2008, Altdorff *et al.* 2016) and volume (Jaenicke *et al.* 2008).

Microtopography is known to affect soil hydrophysical properties in mire ecosystems. A study conducted by Baird *et al.* (2016) found clear patterns in K_s between adjacent hummocks and hollows (microforms) at 0.5 metre depth in a raised bog. Morris *et al.* (2019) also explored the effect of microforms on K_s (vertical and horizontal), and collected samples from hummocks and lawns in a raised bog. They found a strong independent influence of microhabitat on log-transformed vertical K_s. Similarly, Branham & Strack (2014) found K_s to be higher in hummocks than in the hollows at the surface of a *Sphagnum*-dominated fen and bog. Such relationships between microtopography and soil hydrophysical properties have been generally explored in raised and blanket bogs with little to no focus on other mire systems. Thus, there is a gap in our understanding of such relationships in degraded coastal mires following rewetting.

Therefore, the objectives of our study are to (1) understand spatial structures of hydrophysical properties of organic soils, (2) investigate spatial patterns of organic matter accumulation in relation microtopography, and (3) understand the role of the organic horizon with respect to underlying mineral soil with respect to hydrological connectivity, in a coastal flood mire. We also use spatial measurements of hydrophysical properties (K_s and SOM) and soil surface microelevation to make spatial predictions, which has not been done in coastal mires.

METHODS

Study site

The study site lies in the north-eastern German federal state of Mecklenburg-Western Pomerania which is home to around 3000 km^2 of peatlands (13 % of the total land area of the state; Tiemeyer *et al.* 2006). The study site is part of a non-tidal coastal flood mire known as "Karrendorfer Wiesen" and is located (54.1576° N, 13.3860° E) between Greifswald and Stralsund, on a peninsula in the Baltic Sea (Figure 1). Karrendorfer Wiesen has an area of approximately 3.5 km^2 and is a part of the 400 km^2 of coastal peatlands covering the state (Jurasinski *et al.* 2018). It is characterised by weakly undulating ground moraine, which was flooded during postglacial transgressions. Currently it lies within the natural flooding zone of the "Nordmecklenburgschen Bodden" (Bernhardt & Koch 2003). The study site was drained in 1820. In 1850, a dike system was constructed and the area was used intensively as cropland and pasture. The height of the dike was increased between 1971 and 1974. The dike blocked the flow of seawater

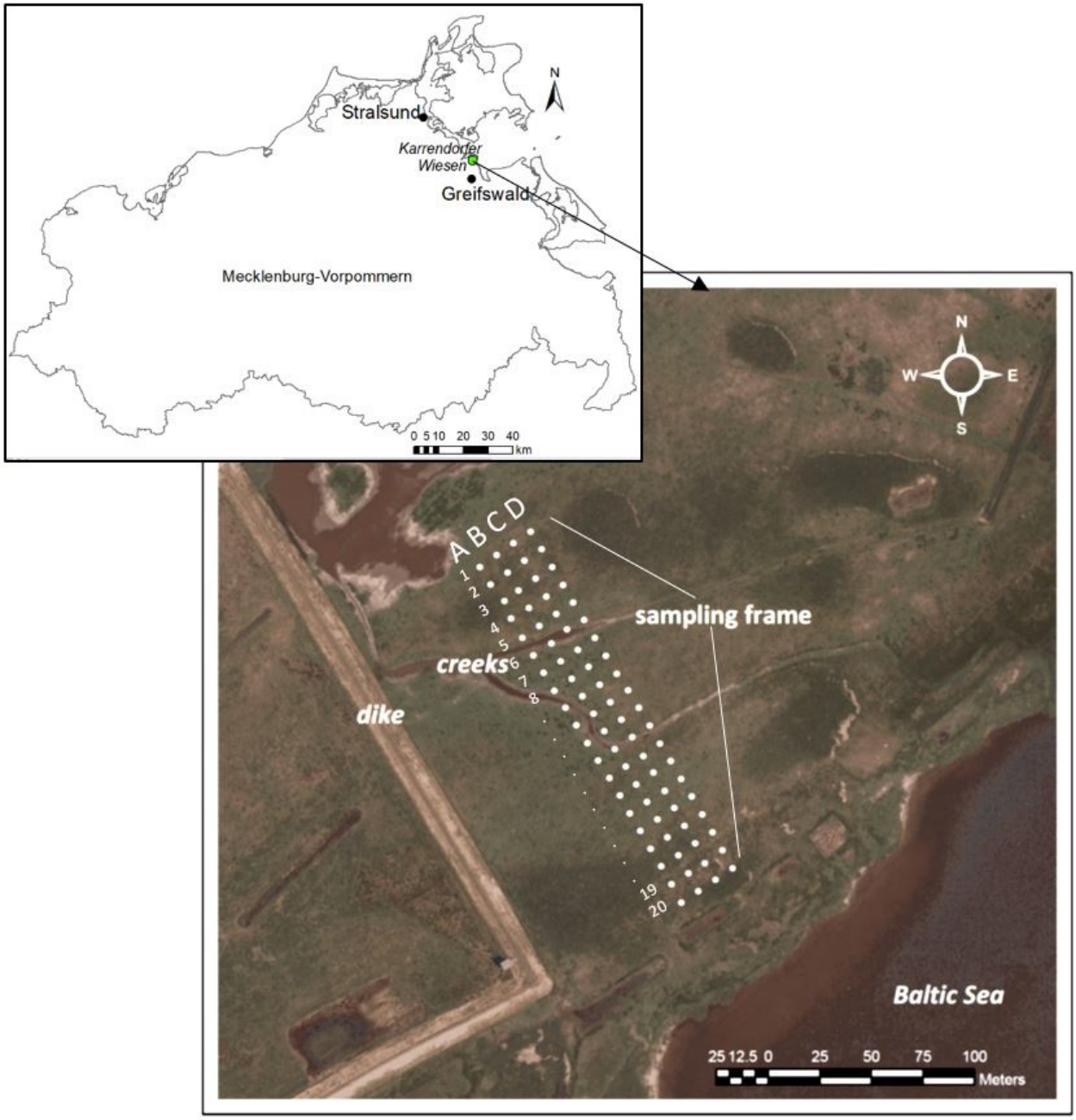

Figure 1. Location of the study area "Karrendorfer Wiesen". The white dots on the map show the locations where soil samples were collected.

flooding to the mires, reducing soil salinity; and the accomplished drainage lowered the water table, accelerating organic matter mineralisation. However, in the early 1990s the area lost its importance as pasture due to a small number of landowners coupled with the poor condition of the old dike system (Lampe & Wolrab 1996). Thus, in 1993 the old dikes were removed and a new dike system was built so as to reinitiate natural flooding dynamics on part of the area (Beyer *et al.* 2019). Currently this area is used as a low-intensity pasture (Bernhardt & Koch 2003, Beyer *et al.* 2019). Karrendorfer Wiesen is recognised as a "National Natural Heritage" by the Federal Government of Germany, and is therefore protected for nature conservation. It is also an important coastal bird sanctuary (Janssen *et al.* 2019, July 16).

The coastal mire is represented by a mosaic of micro-elevational changes consisting of marly till and sandy soils, and interspersed low-lying areas (Bernhardt & Koch 2003) consisting of fen gley soils with 13–28 cm of peat (Janssen *et al.* 2019). Peat is an organic soil which is composed of partially decomposed plants (Kelly *et al.* 2017). According to Rydin & Jeglum (2006) there is no general agreement on how to define peat using organic matter content and its defining range may vary from 20 % to 80 % organic matter by weight. For this reason, coupled with the fact that there is high variance of the percentage of organic matter found in our samples, throughout this article we refer to the soils of this coastal mire as "organic soil" or "peat". The pH of the soil ranges from 4.4 to 6.1 depending on the depth. The soils have a bulk density of around 0.57 g cm^{-3} with a total porosity of 0.71 cm^3 cm^{-3} (Liu & Lennartz 2019b).

According to vegetation data collected by Beyer *et al.* (2019), the study site is characterised by salt marsh species. *Agrostis stolonifera* is the most dominant species followed by *Alopecurus geniculatus* and *Juncus gerardii*. *Elymus repens, Triglochin martima, Deschampsia cespitosa, Trifolium repens* and *Trifolium hybridum* occur sporadically while *Spergularia salina, Poa pratensis, Potentilla anserina, Aster tripolium* and *Plantago maritima* appear less often throughout the study area.

Soil sample collection and saturated hydraulic conductivity determination

The sampling frame covers an area of 6000 m^2 (200 × 30 m). For determining soil organic matter content (SOM), soil samples at a depth of about 15 cm were collected using a gouge auger every 10 metres at 80 points. Prior to soil sample collection, at the same depth, *in situ* saturated hydraulic conductivity (K_s) was measured using a direct-push piezometer with falling head which has been used for peat soils in previous studies (Ronkanen & Kløve 2005, Saarinen *et al.* 2013, Postila *et al.* 2015, Mustamo *et al.* 2016). This device is particularly useful for our study area because laboratory based K_s measurements would require the collection of large amounts of undisturbed soil which is not possible given the protection status of the Karrendorfer Wiesen. Other field methods for measuring K_s such as the piezometer slug test would require extensive installation of piezometer pipes, which is again not feasible given the protection status of the study site. However, K_s could be measured at only 39 points, as it was not possible to penetrate the soil surface at all locations using the device.

The direct-push piezometer (see Figure 2) is inserted into the soil at the desired depth slowly and without any twisting motion to avoid potential smearing. Additionally, a tripod with a clip is used to hold the device in place. Afterwards, water collected from the field site is poured into the reservoir. The hydraulic head is noted after which the control valve at the base of the reservoir is released to allow the water to flow through the pipe. At the tip of the piezometer, there is a meshed opening (the screen) on two sides with a diameter of 2 cm. It is here that the piezometer water comes into contact with the soil. The falling head is timed and recorded. Due to loss of head in the piezometer the method allows for accurate K_s measurements below 0.002 m s^{-1} (Ronkanen & Kløve 2005). Prior to carrying out fieldwork, several *in situ* measurements of K_s using the direct-push piezometer were compared to several laboratory measurements using a constant-head upward-flow permeameter (Liu *et al.* 2016) on undisturbed soil samples collected from the same locations (see Figure A1 in the Appendix). Results from both methods are statistically similar.

The rate of the outflow (q) at the piezometer screen/outlet at any time (t) is proportional to the hydraulic conductivity (K) of the soil and to the unrecovered head difference (H - h) (Hvorslev 1951, Mustamo *et al.* 2016), so that:

$$q(t) = \pi r^2 \frac{\partial h}{\partial t} = FK\,(H - h) \qquad [1]$$

where r = radius of the piezometer reservoir (m), H = water level from outflow point of piezometer (m), h = water level in the reservoir (m), F = 9 (dimensionless), shape factor calculated according to equation provided in Akanegbu (2013), t = time (s).

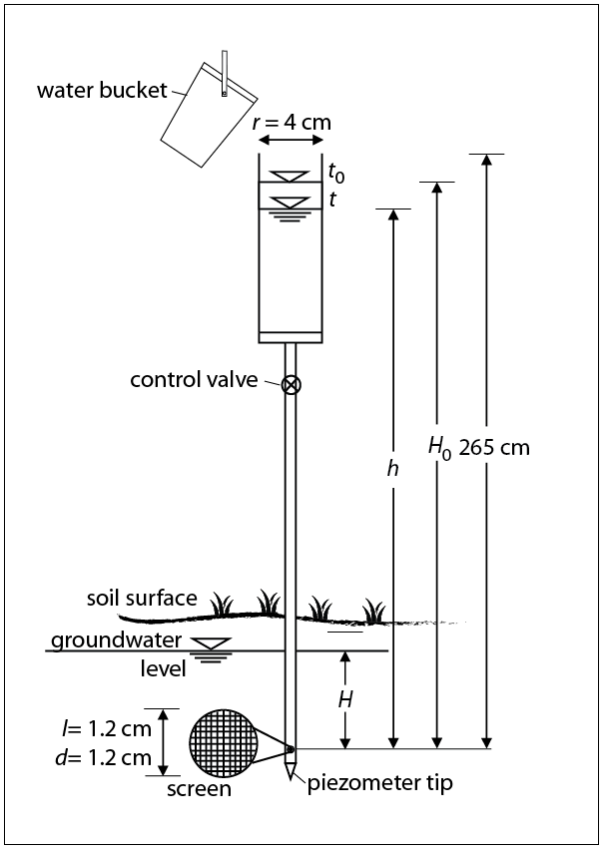

Figure 2. A schematic diagram of a direct-push piezometer with falling head (adapted from Ronkanen & Klove, 2005). Height from the centre of the outlet screen = 265 cm; r (inner radius of the reservoir) = 4.0 cm; length and diameter of the outlet screen = 1.2 cm; H = water level from outflow point of piezometer; H_0 = the initial water level in the reservoir, h = water level in the container at a time point t. The tip of the device is sharp and connected smoothly to the body of the device to avoid compression of soil when inserting into the ground.

From Equation 1 the following equation may be derived:

$$ln\left(\frac{h-H}{H_0-H}\right) = -\frac{FK}{\pi r^2}t \qquad [2]$$

A plot of the left-hand side of Equation 2 against time represents a straight line on a semi-logarithmic graph. Therefore, K can be calculated from the slope of this straight line.

Due to the shallow depth of peat (13–28 cm), it is important to understand the role of the underlying mineral horizon in terms of groundwater flow. Therefore, further soil samples were collected from three locations (B2, B9, and B20; see Figure 1) at depths of 20–40 cm, 40–60 cm, and 60–80 cm for textural analysis.

Laboratory analysis

Soil organic matter content (SOM) was determined by loss-on-ignition according to DIN 18128 (DIN 2002) and expressed as weight percent (%w/w). Advantages of this method are (1) a large number of samples can be run simultaneously and (2) equipment cost is low (De Vos *et al.* 2005). Another prominent method of determining SOM is the Walkley-Black acid digestion method. However, for soils with high organic matter content this method may result in inaccuracies due to incomplete oxidation of organic carbon in the sample (Lefèvre *et al.* 2017).

Additionally, particle size distribution (soil texture) from locations B2, B9 and B20 and three depths of the mineral horizons (20–40, 40–60 and 60–80 cm) was determined using the sieving and sedimentation method according to DIN ISO 11277 (DIN ISO 2002). Prior to soil texture analysis, all samples were tested for carbonates by using 10 % HCl which did not result in any fizzing indicating a lack of significant amounts of carbonates. SEDIMAT 4-12 (UGT), which works on the basis of the KÖHN analysis to DIN ISO 11277, was used to determine the three silt fractions (coarse, medium, fine) and one clay fraction. The remaining sand fractions were further separated using sieves with mesh sizes of 63 µm, 200 µm, and 630 µm.

Elevation data and geostatistical analysis

All sampling locations and corresponding soil surface elevations were recorded using a high precision GNSS receiver (Leica Viva GS08 plus) which uses real-time kinematic positioning. ArcMap 10.5.1 was used to analyse spatial data. Using the Geostatistical Wizard, accessed through Geostatistical Analyst extension, empirical variograms of K_s (log-transformed), SOM and soil surface microtopography (SSM) were generated. Empirical variograms of K_s (log-transformed) and SSM were fitted with Gaussian models, while the variogram of SOM was fitted with a "Stable" model with parameter = 1.898. These variograms were then utilised to generate prediction maps using "simple kriging" method. For calculation of partial sill and nugget, weighted least squares was used. The models and the parameters are described in the Results section (see Table 3).

A "leave-one-out" method was used for cross validation. Each data location is removed, one at a time, and the associated data value is predicted. The predicted and actual values at the location of a

removed point are then compared and this procedure is repeated for a second point, a third and so on. All the measured and predicted values were compared using scatterplots and quantile-quantile plots. Plots of predicted versus observed values of all three variables (K_s, SOM, and SSM) are provided in Figure A2. The maps of prediction standard errors for all three kriged variables are presented in Figure A3.

For understanding the association between observed SOM and K_s and between SOM and SSM, in addition to calculating the conventional Pearson correlation, bivariate Moran's I was computed using GeoDa version 1.12, as it is more suitable for variables with spatial dependencies. Lee (2017) states that bivariate spatial dependence refers to circumstances in which observational units in close proximity hold shared information in terms of their bivariate association, and this violates the assumption of independent sampling. Thus, the shared information spuriously strengthens or weakens the nature of correlation between the two variables under investigation, thereby making any conventional statistical inferences considerably questionable.

Moran's I is a well-known indicator of spatial autocorrelation. Moran's I values range from -1 to 1. A '0' value indicates no spatial autocorrelation (i.e. perfect spatial randomness). A '-1' suggests perfect negative spatial autocorrelation or clustering of dissimilar values (i.e. perfect dispersion) while +1 indicates perfect clustering of similar values or, in other words, high values or low values cluster together (Tu & Xia 2008). Similar to the univariate Moran's I, the bivariate Moran's I can help to understand spatial dependencies but it helps to assess such relationships between two variables instead of one. The bivariate Moran's I can be visualised as the slope in a scatterplot of the spatially lagged values of one variable (e.g. soil organic matter) on the second variable (e.g. soil surface microtopography). If the slope of this scatterplot is significantly different from zero, then there is a bivariate spatial relationship between the two variables (Sridharan *et al.* 2007). The test is based on an assumption of constant mean and a constant variance (Anselin 2019).

RESULTS

Hydrophysical soil properties and soil surface microtopography

The K_s values of investigated soils ranged from 5.56×10^{-9} m s^{-1} to 4.64×10^{-7} m s^{-1}, and had the highest coefficient of variation (CV) = 199.99 %, while the soil organic matter content (SOM) varied from 1.36 to 59.29 wt% with a CV of 56.65 %. SSM had a very low CV of around 24 % and ranged from 223 cm to 918 cm above mean sea level (Table 1).

Soil texture of the underlying mineral horizon

Soil texture analysis of the mineral soils underlying the peat horizon (0–20 cm) at three locations reveals that for almost all the locations and all depths, the soil can be classified as sandy loam (following USDA) and as medium loamy sand according to German soil textural classification (Eckelmann *et al.* 2006). Table 2 provides the detailed results of the texture analysis.

Spatial structure of hydro-physical soil properties and surface microtopography

Variograms provide a measure of the spatial dependence of soil properties. Both soil properties as well as SSM can be observed to be spatially dependent. While log(K_s) follows a Gaussian curve (R^2 = 84.85), SOM follows a Stable model with a parameter of 1.898 (R^2 = 90.93). The semivariance of log(K_s) increases initially and then levels out at a lag distance of 87 m while SOM levels off at a slightly higher lag distance of 100 m (see Figure 3). Therefore, beyond these separation distances the hydro-physical soil properties under investigation are not auto-correlated. Soil surface

Table 1. Summary statistics for hydraulic conductivity (K_s), soil organic matter (SOM) and soil surface microtopography (SSM).

Soil variables	Mean	SD	CV (%)	Minimum	Maximum	*n*
K_s (m s^{-1})	4.17×10^{-8}	8.33×10^{-8}	199.99	5.56×10^{-9}	4.64×10^{-7}	39
SOM (%w/w)	21.36	12.10	56.65	1.36	59.29	80
SSM (m above MSL*)	0.57	0.14	24.56	0.22	0.92	80

**MSL = mean sea level.*

microtopography (SSM) follows a Gaussian curve (R^2 = 93.64), with the semivariance increasing until the range of 53 m and afterwards levels out.

The nugget to sill ratio (NSR) of 57.3 %, 55.2 % for K_s and SOM, respectively, indicates only a moderate spatial autocorrelation (following Cambardella *et al.* 1994) for both soil properties. However, for SSM, a NSR of about 13 % indicates strong spatial autocorrelation (Table 3). Thus, SSM is more strongly autocorrelated than K_s and SOM.

Ideally, at zero separation distance (*h*) the variance should also be zero. However, many soil properties have non-zero variances as *h* tends to zero (Trangmar *et al.* 1985). The variance at zero lag distance is called the nugget effect which represents the local variation occurring at scales finer than the sampling interval, such as those due to sampling error, fine-scale spatial variability and the measurement error. Log(K_s) has a slightly higher nugget effect (0.775) compared to that of SOM (0.698), while SSM has a much smaller nugget effect (0.139) indicating much lower errors and lower fine-scale spatial variability.

Spatial heterogeneity of hydraulic conductivity, SOM and soil surface microtopography

There is a general tendency for K_s to increase in the direction of the sea, with no clear tendencies closer to the inland water bodies (Figure 4A). However, the plot of predicted K_s versus observed K_s shows that predictions of K_s have substantial errors, especially in comparison to the plots of SOM and SSM (see Figure A2). It can be observed that there is higher SOM closer to the centre, while much lower SOM at the West and South East ends of the study area (Figure 4B). The SSM map shows the highest elevation class (0.76–0.92 m) at the edges (West and South East of the map) and the lowest elevation classes (0.22–0.37 m) at or around the centre (Figure 4C). Therefore, the spatial distribution of SOM can be described by the spatial variation in microtopography in the study area. This can be further illustrated by the bivariate association between the two variables (see Figure 5), discussed in the next subsection.

Bivariate spatial dependencies

A significantly moderate and positive Pearson correlation was obtained between log(K_s) and SOM (r = 0.53, p = 0.0008). In terms of bivariate spatial autocorrelation between the two variables, a positive Moran's I was found (Moran's I = 0.1440) which, although low, is still significant (pseudo-p = 0.02, permutations = 999, z = 2.1870).

A negative spatial autocorrelation (Moran's I = -0.2993) between SOM and SSM were found to be significant (pseudo p-value = 0.001, permutations = 999, z = -5.67, weights generated using Queen's contiguity; see Figure 5). This means that both SOM and SSM are significantly and negatively spatially autocorrelated - a decrease in soil surface elevation is associated with an increase in SOM across space. The possible underlying mechanism behind this is discussed in the following section.

Table 2. Soil texture classes according to German classification (Eckelmann *et al.* 2006). The English terms for the German soil classes were used after Bormann (2007).

Location	Depth (cm)	Clay	Silt	Sand	Soil Texture Class (Germany)
B2	20–40	6.80	37.57	55.63	medium silty sand
	40–60	9.26	33.44	57.30	medium loamy sand
	60–80	16.65	28.85	54.50	highly loamy sand
B9	20–40	12.67	36.25	51.08	highly loamy sand
	40–60	5.59	24.70	69.70	slightly loamy sand
	60–80	10.36	23.95	65.69	medium loamy sand
B20	20–40	10.01	27.94	62.04	medium loamy sand
	40–60	11.14	27.31	61.55	medium loamy sand
	60–80	8.87	20.89	70.24	medium loamy sand

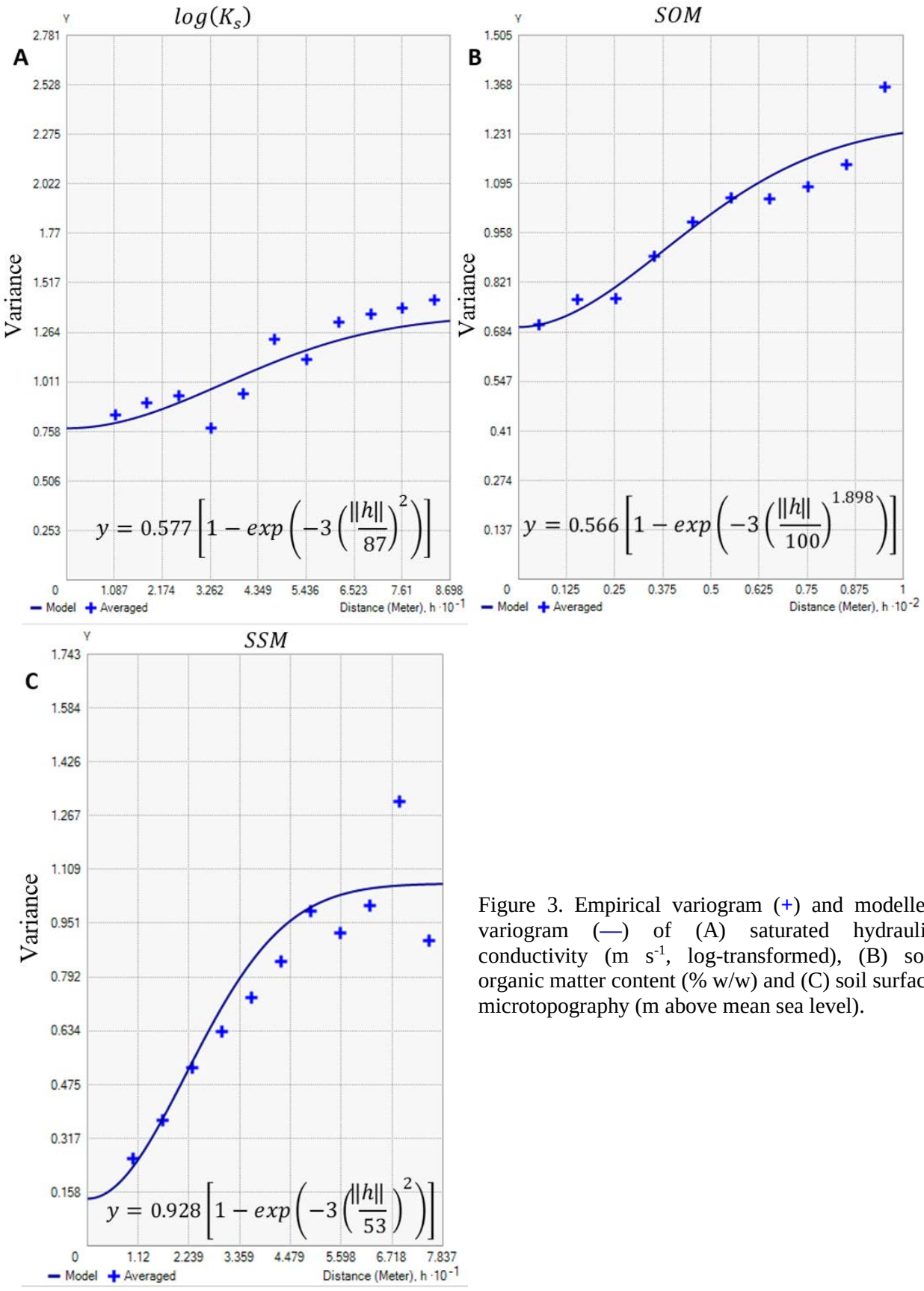

Figure 3. Empirical variogram (+) and modelled variogram (—) of (A) saturated hydraulic conductivity (m s^{-1}, log-transformed), (B) soil organic matter content (% w/w) and (C) soil surface microtopography (m above mean sea level).

Table 3. Variogram models and parameters for SOM and log(K_s).

Soil property	Model	Nugget (C_0)	Sill (C_0+C)	Partial sill (C)	C_0/ C_0+C (%)	Range (m)	R^2 (%)
Log(K_s)	Gaussian	0.775	1.352	0.577	57.322	87	84.85
SOM	Stable (Parameter = 1.898)	0.698	1.264	0.566	55.222	100	90.93
SSM	Gaussian	0.139	1.067	0.928	13.027	53	93.64

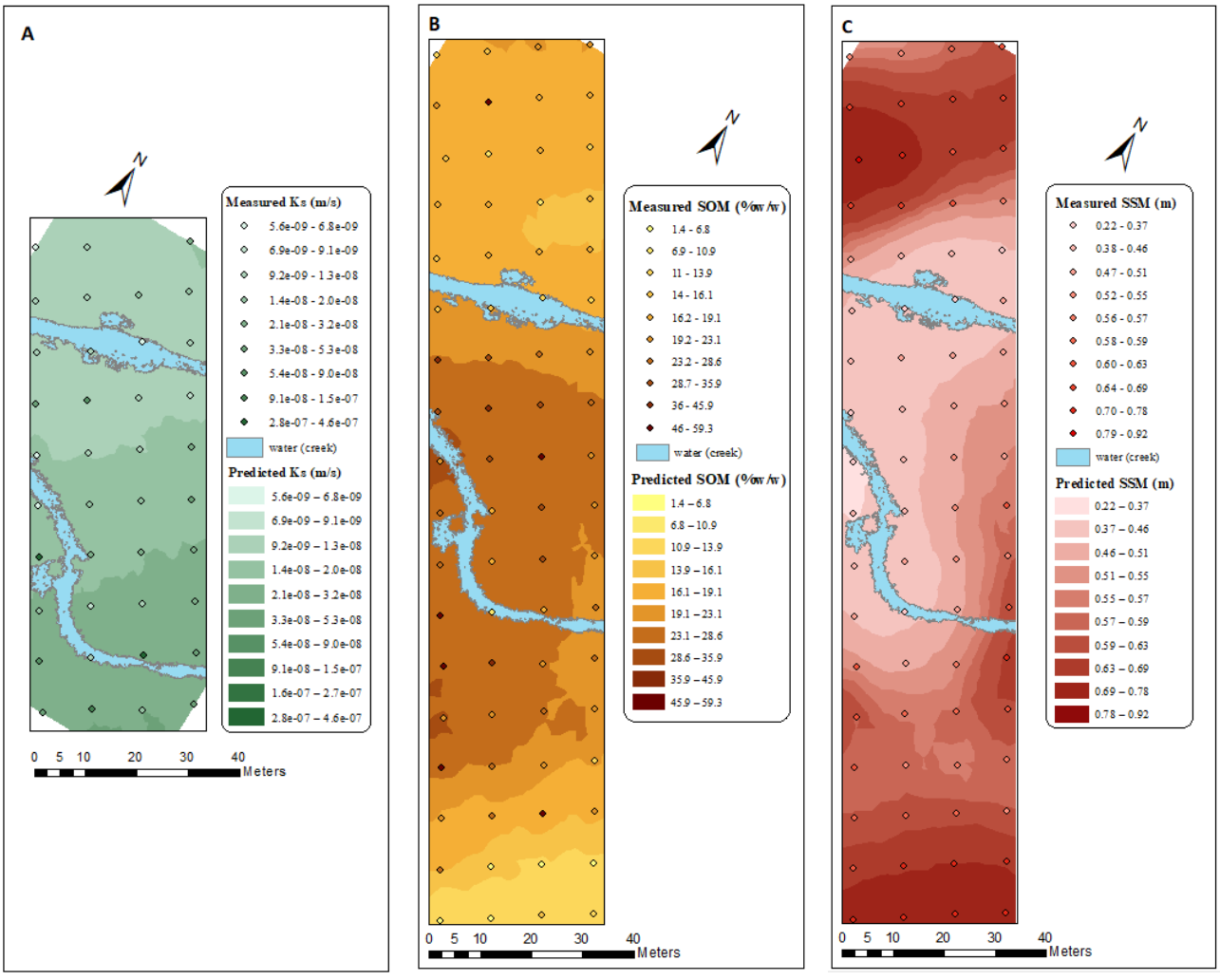

Figure 4. Contour maps showing spatial distribution of (A) K_s (m s^{-1}), (B) SOM (%w/w) and (C) SSM (in metres above mean sea level).

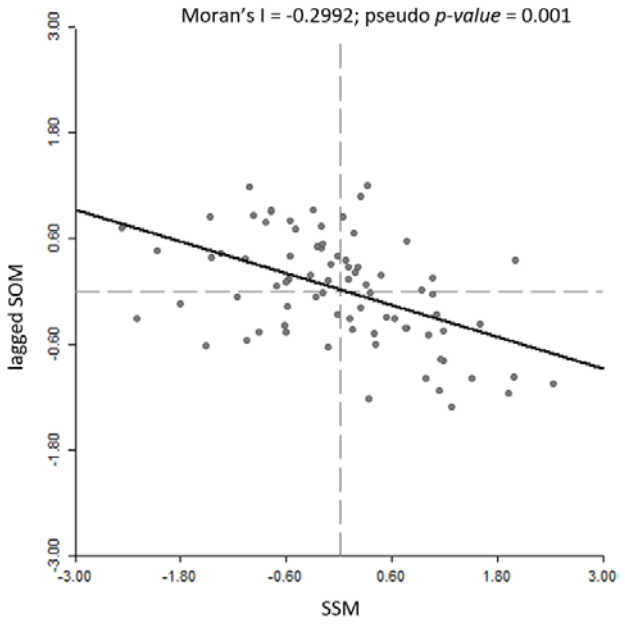

Figure 5. Bivariate Moran's I showing the spatial relationship between observed soil surface microtopography (micro-elevation) and observed soil organic matter content (lagged).

DISCUSSION

Compared to mineral soils, organic soils of coastal flood mires are less studied, especially in relation to space and microtopography. Our study investigates existing spatial structures and patterns of soil hydrophysical properties such as SOM and K_s and how microtopography may affect such properties. Understanding spatial patterns of the accumulation of SOM and distribution of K_s and how they are modified by surface microtopography in such mire ecosystems are of particular interest since formation of peat and maintaining hydrological connectivity are prerequisites for the effective restoration of mire and peatland ecosystems.

Analysis of SOM of the topsoil (organic horizon) reveals that the coastal flood mire has a mean SOM of 21.4 % (SD = 12.1 %), ranging from 14 % to around 60 %, with a CV of 57 % which is indicative of a very high variation following Warrick (1980) and Paz Ferreiro *et al.* (2016). For mineral soils, Bernardi *et al.* (2017) reports a substantially lower CV for SOM, of around 15 %, while Paz Ferreiro *et al.* (2016) reports CV ranging from 27 % to 40 % (depending on soil depth and land use). For peat soils of a drained wetland located in the Qinghai-Tibet plateau of China, Bai *et al.* (2010) reports a CV of 9 % for soil organic carbon which is a substantially lower variation than that of the current study. Land use can also have an effect on the variation of soil organic matter in peat soils with CV ranging between 109 % in arable peat, 68 % in woodland peat, 45 % in grassland peat and 38 % in moorland peat according to a study carried out in south-west England (Glendell *et al.* 2014).

For the organic horizon of the study site, the mean K_s is 4×10^{-8} m s^{-1} (SD = 8×10^{-8} m s^{-1}) with a minimum of 6×10^{-9} m s^{-1} to a maximum of 5×10^{-7} m s^{-1}. Our values of K_s are very low, about 2 to 4 orders of magnitude lower than that estimated by van Dijk *et al.* (2017) for peat sediments in a coastal wetland of the Netherlands (around 7×10^{-5} m s^{-1}). K_s shows a very high variation, with a CV of about 200 percent which is consistent with values reported for peat soils (CV = 282 %, calculated from a meta-analytical study by Liu & Lennartz 2019a).

Soil organic matter content and K_s (log-transformed) were found to be significantly and positively correlated, but only moderately (r = 0.53, p = 0.0008). A positive correlation as such is consistent with the results of several other studies, including those for mineral soils (Hur *et al.* 2009, Zare *et al.* 2010, Nath & Krishna 2014) as well as for organic soils (Liu & Lennartz 2019a). Macroporosity is a major factor controlling K_s (Liu *et al.* 2016). Liu & Lennartz (2019a) found that macroporosity is higher in peat with high organic matter content than in soils with low organic matter content.

In terms of spatial dependencies in our study, K_s and SOM are spatially autocorrelated with each other with a significant and positive Moran's I (Moran's I = 0.1440, p = 0.02), suggesting non-randomness in their overall spatial pattern. Both K_s and SOM show moderate spatial autocorrelation as defined by Cambardella *et al.* (1994), with a range of about 87 m for K_s and 100 m for SOM. For mineral soils Zeleke & Bing (2005) report a much lower spatial range of about 50 m for K_s and 43 m for organic carbon. Paz Ferreiro *et al.* (2016) investigated the spatial variability of mineral soil properties according to different land uses and depth, and also found much lower spatial ranges with a minimum of around 12 m to a maximum of about 60 m, depending on land use and soil depth. However, the predicted map of K_s should be interpreted with caution, as the plot of predicted values against observed values show poor prediction performance which may be attributable to (1) small sample size (n = 39) and (2) large sample intervals (10 m). This was not the case for the prediction of SOM, which performed much better, while SSM prediction performed the best among all three variables. This may be an indication that K_s follows

spatial patterns at much smaller scales than SOM and SSM in coastal mires as it has also been observed from the variograms (Figure 3). Although a sampling interval of 10 m allowed us to have larger spatial coverage, it may have resulted in an increased nugget effect especially for the prediction of K_s. Follow-up studies should incorporate nested sampling of different interval lengths, to understand multiple scales at which soil physical properties and soil surface microtopography interact in coastal mires.

A key finding of our research is that SOM and soil-surface microtopography (SSM, micro-elevation) are significantly negatively autocorrelated (Moran's I = 0.2993, p = 0.001), which can also be visually observed by comparing the kriged map of SOM with the map of SSM. The SOM map predicts higher organic matter content in the centre of the ecosystem at lower elevations, while at the edges of the study area, at higher elevations, SOM decreases. Local depressions in the centre of the ecosystem provide a wetter and therefore a more anaerobic environment as oxygen diffuses 10,000 times slower through water than it does through air and in the presence of waterlogged decomposing plant material the supply of oxygen is rapidly depleted (Clymo 1983, Lindsay & Andersen 2016). Thus, under anaerobic conditions, carbon mineralisation rate decreases, enabling the accumulation of organic matter, as has been confirmed by a multitude of studies (Aerts & Ludwig 1997, Yavitt *et al.* 1997, Öquist & Sundh 1998, Kettunen *et al.* 1999, Blodau *et al.* 2004, Benavides 2015). However, unlike our study, most of these studies were based on laboratory experiments and not on field research. We may therefore generalise that SSM is an important feature to take into account while planning restoration measures especially when there is lack of water table monitoring with high spatial resolution and when addressing coastal mires with low K_s, located at the Baltic Sea coast - where soils are not subjected to significant tidal flooding.

For almost all three locations and for all depths (of the underlying mineral horizons), the soil can be characterised as sandy loam (USDA classification) which, according to Schaap *et al.* (2001), has an average K_s of about 4×10^{-6} m s^{-1} (SD = 5×10^{-7} m s^{-1}). Therefore, even the maximum *in situ* K_s (5×10^{-8} m s^{-1}) of the organic horizon is two orders of magnitude lower than that of the underlying mineral horizon, which is an indication that the organic horizon with its relatively low hydraulic conductivity acts as a hydrological barrier, at least in terms of infiltration. This finding is consistent with a study carried out on a different Baltic coastal peatland which found that the peat layer has K_s ranging from 1×10^{-6} to 1×10^{-8} m s^{-1} which is one to two orders of magnitude lower than that of the underlying mineral soil with a K_s of 2×10^{-5} to 6×10^{-5} m s^{-1} (Ibenthal 2019). This brings to the fore the question of whether the organic soil or peat horizon of other coastal wetlands which developed under similar conditions also acts as a hydrological barrier.

In terms of rewetting, it is therefore useful to know locations with higher microelevations because these are potential hotspots for faster degradation rates as flooding or rainfall events may lead to water accumulating in areas of low micro-elevation only, through overland flow or inflow through the existing creek system. Furthermore, during rainfall events which lead to a rise in groundwater level, areas with lower elevations will become saturated first, and only afterwards the water table may reach higher elevations. In situations where restoration projects utilise water level monitoring wells, data on micro-elevation may inform locations where installations should be set up. In addition, the low hydraulic conductivity of the degraded peat in the presence of lower micro-elevations in the centre of the ecosystem is likely to increase the residence time of floodwater and thus may enable (new) peat accumulation. Thus, we conclude that for the restoration of non-tidal coastal mires, where flooding events are not as frequent, K_s and SSM are even more important factors to consider than for tidal systems. Extensive research in such under-studied and complex ecosystems is required in order to better understand the underlying mechanisms of peat formation following dike removal (rewetting).

ACKNOWLEDGEMENTS

The authors thank Johanna Blossei, Miaorun Wang Tilo Hartwig and Laurenz Teuber for helping with data collection and logistics; Evelyn Bolzmann for providing guidance on the laboratory analysis; Matthias Naumann for providing support with high precision GPS; Görres Grenzdörffer, Donald Myers and Shajratul Alam for their valuable advice on geospatial analysis; and Lennart Gosch for German language support. The European Social Fund (ESF) and the Ministry of Education, Science and Culture of Mecklenburg-Western Pomerania funded this work within the project WETSCAPES (ESF/14-BM-A55-0028/16). Financial support was also received from the Research Training Group Baltic TRANSCOAST program, funded by the DFG (Deutsche Forschungsgemeinschaft) under Grant Number DFG-GRK 2000/1.

AUTHOR CONTRIBUTIONS

HL, SA and BL conceived the research idea and design. SA undertook the field measurements and laboratory analysis. BK provided the direct-push piezometer. SA analysed the data and designed the Figures with input from FB. SA wrote the first draft while all authors discussed the results and revised the manuscript.

REFERENCES

Adams, W.A. (1973) The effect of organic matter on the bulk and true densities of some uncultivated podzolic soils. *Journal of Soil Science*, 24, 10–17.

Aerts, R., Ludwig, F. (1997) Water-table changes and nutritional status affect trace gas emissions from laboratory columns of peatland soils. *Soil Biology and Biochemistry*, 29, 1691–1698.

Akanegbu, O. 2013 *Comparison of Different Methods of Measuring Hydraulic Conductivity in Drained Peat Soils Using DRAINMOD as a Verification Tool*. Master Thesis, University of Oulu, Oulu, Finland, 116 pp.

Altdorff, D., Bechtold, M., van der Kruk, J., Vereecken, H., Huisman, J.A. (2016) Mapping peat layer properties with multi-coil offset electromagnetic induction and laser scanning elevation data. *Geoderma*, 261, 178–189.

Anselin, L. (2019) Global spatial autocorrelation (2): bivariate, differential and EB rate Moran scatter plot. *GeoDa Workbook*. Online at: https://geodacenter.github.io/workbook/5b_global_adv/lab5b.html.

Bai, J., Ouyang, H., Xiao, R., Gao, J., Gao, H., Cui, B., Huang, L. (2010) Spatial variability of soil carbon, nitrogen, and phosphorus content and storage in an alpine wetland in the Qinghai-Tibet Plateau, China. *Australian Journal of Soil Research*, 48, 730–736.

Baird, A.J., Milner, A.M., Blundell, A., Swindles, G.T., Morris, P.J. (2016) Microform-scale variations in peatland permeability and their ecohydrological implications. *Journal of Ecology*, 104, 531–544.

Beilman, D.W., Vitt, D.H., Bhatti, J.S., Forest, S. (2008) Peat carbon stocks in the southern Mackenzie River Basin: Uncertainties revealed in a high-resolution case study. *Global Change Biology*, 14, 1221–1232.

Benavides, J.C. (2015) The effect of drainage on organic matter accumulation and plant communities of high-altitude peatlands in the Colombian tropical Andes. *Mires and Peat*, 15, 01, 15 pp.

Benscoter, B.W., Vitt, D.H., Wieder, R.K. (2005) Association of postfire peat accumulation and microtopography in boreal bogs. *Canadian Journal of Forest Research*, 35, 2188–2193.

Bernardi, A.d.C., Bettiol, G.M., Mazzuco, G.G., Esteves, S.N., Oliveira, P.P.A., Pezzopane, J.R.M. (2017) Spatial variability of soil fertility in an integrated crop livestock forest system. *Advances in Animal Biosciences*, 8, 590–593.

Bernhardt, K.G., Koch, M. (2003) Restoration of a salt marsh system: temporal change of plant species diversity and composition. *Basic and Applied Ecology*, 4, 441–451.

Bevington, J., Piragnolo, D., Teatini, P., Vellidis, G., Morari, F. (2016) On the spatial variability of soil hydraulic properties in a Holocene coastal farmland. *Geoderma*, 262, 294–305.

Beyer, F., Jurasinski, G., Couwenberg, J., Grenzdörffer, G. (2019) Multisensor data to derive peatland vegetation communities using a fixed-wing unmanned aerial vehicle. *International Journal of Remote Sensing*, 40(24), 9103–9125.

Blodau, C., Basiliko, N., Moore, T.R. (2004) Carbon turnover in peatland mesocosms exposed to different water table levels. *Biogeochemistry*, 67, 331–351.

Boelter, D.H. (1969) Physical properties of peats as related to degree of decomposition 1. *Soil Science Society of America Journal*, 33, 606–609.

Bormann, H. (2007) Analysis of the suitability of the German soil texture classification for the regional scale application of physical based hydrological model. *Advances in Geosciences*, 11, 7–13.

Brandyk, T., Szatylowicz, J., Oleszczuk, R., Gnatowski, T., Parent, L.É., Ilnicki, P. (2002) Water-related physical attributes of organic soils. In: Ilnicki, P., Parent, L.E. (eds.) *Organic Soils and Peat Materials for Sustainable Agriculture*, CRC Press, Boca Raton, 33–66.

Branham, J.E., Strack, M. (2014) Saturated hydraulic conductivity in *Sphagnum*-dominated peatlands: do microforms matter? *Hydrological Processes*, 28, 4352–4362.

Cambardella, C.A., Moorman, T.B., Novak, J.M., Parkin, T.B., Karlen, D.L., Turco, R.F., Konopka, A.E. (1994) Field-scale variability of soil properties in central Iowa soils. *Soil Science Society of America Journal*, 58, 1501–1511.

Chmura, G.L., Anisfeld, S.C., Cahoon, D.R., Lynch, J.C. (2003) Global carbon sequestration in tidal,

saline wetland soils. *Global Biogeochemical Cycles*, 17(4), 1111, 12 pp.

Clymo, R.S. (1983) Peat. In: Goodall, D.W., Gore, A.J.P. (eds.) *Mires: Swamp, Bog, Fen and Moor - Regional Studies*, Ecosystems of the World 4B, Elsevier, Amsterdam, 159–224.

Dargie, G.C., Lewis, S.L., Lawson, I.T., Mitchard, E.T.A., Page, S.E., Bocko, Y.E., Ifo, S.A. (2017) Age, extent and carbon storage of the central Congo Basin peatland complex. *Nature*, 542, 86–90.

De Vos, B., Vandecasteele, B., Deckers, J., Muys, B. (2005) Capability of loss-on-ignition as a predictor of total organic carbon in non-calcareous forest soils. *Communications in Soil Science and Plant Analysis*, 36, 2899–2921.

DIN (2002) Soil - Investigation and testing - Determination of ignition loss. DIN 18128:2002-12, Beuth, Berlin.

DIN ISO (2002) 11277: Soil quality - Determination of particle size distribution in mineral soil material - Method by sieving and sedimentation. 11277:2002-08, Beuth, Berlin.

Eckelmann, W., Sponagel, H., Grottenthaler, W., Hartmann, K.-J., Hartwich, R., Janetzko, P., Joisten, H., Kühn, D., Sabel, K.-J., Traidl, R. (eds.) (2006) *Bodenkundliche Kartieranleitung. KA5* (*Manual of Soil Mapping. 5th Ed. (KA5)*), Schweizerbart'sche Verlagsbuchhandlung, Hannover, 438 pp.

Fox, D.M., Le Bissonnais, Y., Quétin, P. (1998) The implications of spatial variability in surface seal hydraulic resistance for infiltration in a mound and depression microtopography. *Catena*, 32, 101–114.

Glendell, M., Granger, S.J., Bol, R., Brazier, R.E. (2014) Quantifying the spatial variability of soil physical and chemical properties in relation to mitigation of diffuse water pollution. *Geoderma*, 214-215, 25–41.

Grover, S.P.P., Baldock, J.A. (2013) The link between peat hydrology and decomposition: Beyond von Post. *Journal of Hydrology*, 479, 130–138.

Heller, C., Zeitz, J. (2012) Stability of soil organic matter in two northeastern German fen soils: The influence of site and soil development. *Journal of Soils and Sediments*, 12, 1231–1240.

Henman, J., Poulter, B. (2008) Inundation of freshwater peatlands by sea level rise: Uncertainty and potential carbon cycle feedbacks. *Journal of Geophysical Research: Biogeosciences*, 113, G01011, 11 pp.

Holden, J., Burt, T.P. (2003) Runoff production in blanket peat covered catchments. *Water Resources Research*, 39(7), 1191, 9 pp.

Holden, J., Chapman, P.J., Labadz, J.C. (2004) Artificial drainage of peatlands: Hydrological and hydrochemical process and wetland restoration. *Progress in Physical Geography*, 28, 95–123.

Holden, J., Evans, M.G., Burt, T.P., Horton, M. (2006) Impact of land drainage on peatland hydrology. *Journal of Environmental Quality*, 35, 1764–1778.

Hur, S.-O., Jung, K.-H., Sonn, Y.-K., Ha, S.-K., Kim, J.-G. (2009) Determination of pedo-transfer function using the relation between soil particle distribution, organic matter and water movement in soil originated from limestone. *Korean Journal of Soil Science and Fertilizer*, 42, 132–138.

Hvorslev, M.J. (1951) *Time Lag and Soil Permeability in Ground-water Observations*. Bulletin 36, Waterways Experiment Station, U.S. Army Corps of Engineers, Vicksburg, Mississippi, 55 pp.

Ibenthal, M. (2019) *Marine and Terrestrial Influence on Submarine Groundwater Discharge in Coastal Waters Connected to a Peatland.* Doctoral thesis, Georg-August-Universität Göttingen, Germany, 135 pp.

Jaenicke, J., Rieley, J.O., Mott, C., Kimman, P., Siegert, F. (2008) Determination of the amount of carbon stored in Indonesian peatlands. *Geoderma*, 147, 151–158.

Janssen, M., Böttcher, M.E., Brede, M., Burchardt, H., Forster, S., Karsten, U., Leinweber, P., Lennartz, B., Rehder, G., Schubert, H., Schulz-Vogt, H., Sokolova, I.M., Voss, M., Jurasinski, G. (2019) The Baltic TRANSCOAST approach - investigating shallow coasts as terrestrial-marine interface of water and matter fluxes. *EarthArXiv* (non-peer reviewed preprint, last edited Jul 16, 2019), doi:10.31223/osf.io/e7cj2. Online at: https://eartharxiv.org/discover?q=janssen, accessed 14 Feb 2020.

Joosten, H. (2010) *The Global Peatland CO_2 Picture: Peatland Status and Drainage Related Emissions in all Countries of the World*. Wetlands International, Ede, 43 pp.

Jurasinski, G., Janssen, M., Voss, M., Böttcher, M.E. and 26 others (2018) Understanding the coastal ecocline: Assessing sea-land interactions at non-tidal, low-lying coasts through interdisciplinary research. *Frontiers in Marine Science*, 5, 342, 22 pp.

Kechavarzi, C., Dawson, Q., Leeds-Harrison, P.B. (2010) Physical properties of low-lying agricultural peat soils in England. *Geoderma*,

154, 196–202.

Kelly, T.J., Lawson, I.T., Cole, L.E.S. (2017) Peat. In: White, W.M. (ed.) *Encyclopedia of Geochemistry: A Comprehensive Reference Source on the Chemistry of the Earth*. Springer International Publishing, Cham, 1–4.

Kettunen, A., Kaitala, V., Lehtinen, A., Lohila, A., Alm, J., Silvola, J., Martikainen, P.J. (1999) Methane production and oxidation potentials in relation to water table fluctuations in two boreal mires. *Soil Biology and Biochemistry*, 31, 1741–1749.

Kluge, B., Wessolek, G., Facklam, M., Lorenz, M., Schwärzel, K. (2008) Long-term carbon loss and CO_2-C release of drained peatland soils in northeast Germany. *European Journal of Soil Science*, 59, 1076–1086.

Lampe, R., Wolrab, B. (1996) Geländeklimatologische und hydrologische Untersuchungen. *Natur und Naturschutz in Mecklenburg-Vorpommern*, 32, 43–55.

Lee, S.-I. (2017) Correlation and spatial autocorrelation. In: Shekhar, S., Xiong, H., Zhou, X. (eds.) *Encyclopedia of GIS*, Springer International Publishing, Cham, 360–368.

Lefèvre, C., Rekik, F., Alcantara, V., Wiese, L. (2017) *Soil Organic Carbon: the Hidden Potential*. Food and Agriculture Organization of the United Nations (FAO), Rome, 77 pp.

Leifeld, J., Menichetti, L. (2018) The underappreciated potential of peatlands in global climate change mitigation strategies. *Nature Communications*, 9, 1–7.

Lewis, C., Albertson, J., Xu, X., Kiely, G. (2012) Spatial variability of hydraulic conductivity and bulk density along a blanket peatland hillslope. *Hydrological Processes*, 26, 1527–1537.

Li, Z., Chen, Z. (2012) Comparing two measuring methods of soil microtopography. In: *2012 First International Conference on Agro-Geoinformatics (Agro-Geoinformatics)*, 1–4.

Lindsay, R., Andersen, R. (2016) Peat. In: Finlayson, C.M., Milton, G.R., Prentice, R.C., Davidson, N.C. (eds.) *The Wetland Book II: Distribution, Description and Conservation*, Springer Netherlands, Dordrecht, 1–6.

Liu, H., Lennartz, B. (2019a) Hydraulic properties of peat soils along a bulk density gradient—A meta study. *Hydrological Processes*, 33, 101–114.

Liu, H., Lennartz, B. (2019b) Short term effects of salinization on compound release from drained and restored coastal wetlands. *Water*, 11, 1549, 13 pp.

Liu, H., Janssen, M., Lennartz, B. (2016) Changes in flow and transport patterns in fen peat following soil degradation. *European Journal of Soil Science*, 67, 763–772.

Ma, Y., Minasny, B., Malone, B.P., Mcbratney, A.B. (2019) Pedology and digital soil mapping (DSM). *European Journal of Soil Science*, 70, 216–235.

Minasny, B., Berglund, Ö., Connolly, J., Hedley, C., de Vries, F., Gimona, A., Kempen, B., Kidd, D., Lilja, H., Malone, B., McBratney, A., Roudier, P., O'Rourke, S., Rudiyanto, Padarian, J., Poggio, L., ten Caten, A., Thompson, D., Tuve, C., Widyatmanti, W. (2019) Digital mapping of peatlands - A critical review. *Earth-Science Reviews*, 196, 102870, 38 pp.

Morris, P.J., Baird, A.J., Eades, P.A., Surridge, B.W.J. (2019) Controls on near-surface hydraulic conductivity in a raised bog. *Water Resources Research*, 55(2), 1531–1543.

Mustamo, P., Hyvarinen, M., Ronkanen, A.-K., Klove, B. (2016) Physical properties of peat soils under different land use options. *Soil Use and Management*, 32, 400–410.

Nath, T.N., Krishna, B.G. (2014) Influence of soil texture and total organic matter content on soil hydraulic conductivity of some selected Tea growing soils in Dibrugarh district of Assam, India. *Journal of International Research*, 1(1), 2–9.

Öquist, M., Sundh, I. (1998) Effects of a transient oxic period on mineralization of organic matter to CH_4 and CO_2 in anoxic peat incubations. *Geomicrobiology Journal*, 15, 325–333.

Page, S.E., Rieley, J.O., Banks, C.J. (2011) Global and regional importance of the tropical peatland carbon pool. *Global Change Biology*, 17, 798–818.

Paz Ferreiro, J., Pereira De Almeida, V., Alves, M.C., Aparecida De Abreu, C., Vieira, S.R., Vidal Vázquez, E. (2016) Spatial variability of soil organic matter and cation exchange capacity in an oxisol under different land uses. *Communications in Soil Science and Plant Analysis*, 47, 75–89.

Perie, C., Ouimet, R. (2008) Organic carbon, organic matter and bulk density relationships in boreal forest soils. *Canadian Journal of Soil Science*, 88, 315–325.

Postila, H., Ronkanen, A.-K., Marttila, H., Kløve, B. (2015) Hydrology and hydraulics of treatment wetlands constructed on drained peatlands. *Ecological Engineering*, 75, 232–241.

Rawls, W.J. (2004) Effect of soil organic carbon on soil hydraulic properties. In: Pachepsky, Y., Rawls, W.J. (eds.) *Development of Pedotransfer*

Functions in Soil Hydrology, Developments in Soil Science 30, Elsevier, Amsterdam, 95–114.

Rezanezhad, F., Price, J.S., Quinton, W.L., Lennartz, B., Milojevic, T., Van Cappellen, P. (2016) Structure of peat soils and implications for water storage, flow and solute transport: A review update for geochemists. *Chemical Geology*, 429, 75–84.

Rogers, K., Kelleway, J.J., Saintilan, N., Megonigal, J.P., Adams, J.B., Holmquist, J.R., Lu, M., Schile-Beers, L., Zawadzki, A., Mazumder, D., Woodroffe, C.D. (2019) Wetland carbon storage controlled by millennial-scale variation in relative sea-level rise. *Nature*, 567, 91–95.

Ronkanen, A.-K., Kløve, B. (2005) Hydraulic soil properties of peatlands treating municipal wastewater and peat harvesting runoff. *Suo*, 56, 43–56.

Rudiyanto, Minasny, B., Setiawan, B.I., Saptomo, S.K., Mcbratney, A.B. (2018) Open digital mapping as a cost-effective method for mapping peat thickness and assessing the carbon stock of tropical peatlands. *Geoderma*, 313, 25–40.

Rydin, H., Jeglum, J.K. (2006) *The Biology of Peatlands*, Oxford University Press, Oxford, 398 pp.

Saarinen, T., Mohammadighavam, S., Marttila, H., Klove, B. (2013) Impact of peatland forestry on runoff water quality in areas with sulphide-bearing sediments; how to prevent acid surges. *Forest Ecology and Management*, 293, 17–28.

Säurich, A., Tiemeyer, B., Dettmann, U., Don, A. (2019) How do sand addition, soil moisture and nutrient status influence greenhouse gas fluxes from drained organic soils? *Soil Biology and Biochemistry*, 135, 71–84.

Schaap, M.G., Leij, F.J., van Genuchten, M.T. (2001) ROSETTA: a computer program for estimating soil hydraulic parameters with hierarchical pedotransfer functions. *Journal of Hydrology*, 251, 163–176.

Scharlemann, J.P.W., Tanner, E.V.J., Hiederer, R., Kapos, V. (2014) Global soil carbon: Understanding and managing the largest terrestrial carbon pool. *Carbon Management*, 5, 81–91.

Schrautzer, J., Sival, F., Breuer, M., Runhaar, H., Fichtner, A. (2013) Characterizing and evaluating successional pathways of fen degradation and restoration. *Ecological Indicators*, 25, 108–120.

Sridharan, S., Tunstall, H., Lawder, R., Mitchell, R. (2007) An exploratory spatial data analysis approach to understanding the relationship between deprivation and mortality in Scotland. *Social Science & Medicine*, 65, 1942–1952.

Tiemeyer, B., Kahle, P. (2014) Nitrogen and dissolved organic carbon (DOC) losses from an artificially drained grassland on organic soils. *Biogeosciences*, 11, 4123–4137.

Tiemeyer, B., Lennartz, B., Vegelin, K. (2006) Hydrological modelling of a re-wetted peatland on the basis of a limited dataset for water management. *Journal of Hydrology*, 325, 376–389.

Trangmar, B.B., Yost, R.S., Uehara, G. (1985) Application of geostatistics to spatial studies of soil properties. *Advances in Agronomy*, 38, 45–94.

Tu, J., Xia, Z.G. (2008) Examining spatially varying relationships between land use and water quality using geographically weighted regression I: Model design and evaluation. *Science of the Total Environment*, 407, 358–378.

van der Ploeg, M.J., Appels, W.M., Cirkel, D.G., Oosterwoud, M.R., Witte, J.P.M., van der Zee, S.E.A.T.M. (2012) Microtopography as a driving mechanism for ecohydrological processes in shallow groundwater systems. *Vadose Zone Journal*, 11, 52–62.

van Dijk, G., Nijp, J.J., Metselaar, K., Lamers, L.P.M., Smolders, A.J.P. (2017) Salinity-induced increase of the hydraulic conductivity in the hyporheic zone of coastal wetlands. *Hydrological Processes*, 31, 880–890.

Warrick, A.W. (1980) Spatial variability of soil physical properties in the field. In: Hillel, D. (ed.) *Applications of Soil Physics*, Academic Press, London, 319–344.

Whittle, A., Gallego-Sala, A.V. (2016) Vulnerability of the peatland carbon sink to sea-level rise. *Scientific Reports*, 6, 28758, 11 pp.

Yavitt, J.B., Williams, C.J., Wieder, R.K. (1997) Production of methane and carbon dioxide in peatland ecosystems across North America: effects of temperature, aeration, and organic chemistry of peat. *Geomicrobiology Journal*, 14, 299–316.

Yu, Z., Loisel, J., Brosseau, D.P., Beilman, D.W., Hunt, S.J. (2010) Global peatland dynamics since the Last Glacial Maximum. *Geophysical Research Letters*, 37, L13402, 5 pp.

Zare, M., Afyuni, M., Abbaspour, K.C. (2010) Effects of biosolids application on temporal variations in soil physical and unsaturated hydraulic properties. *Journal of Residuals Science and Technology*, 7, 227–235.

Zeitz, J., Velty, S. (2002) Soil properties of drained and rewetted fen soils. *Journal of Plant Nutrition and Soil Science*, 165, 618–626.

Zeleke, T.B., Bing, C.S. (2005) Scaling relationships between saturated hydraulic conductivity and soil physical properties. *Soil Science Society of America Journal*, 69, 1691–1702.

Zhang, B.J., Zhang, G.H., Yang, H.Y., Wang, H., Li, N.N. (2018) Soil erodibility affected by vegetation restoration on steep gully slopes on the Loess Plateau of China. *Soil Research*, 56, 712–723.

Zheng, L., Xu, J., Tan, Z., Xu, L., Wang, X. (2019) Spatial distribution of soil organic matter related to microtopography and NDVI changes in Poyang Lake, China. *Wetlands*, 39, 1–13.

Submitted 23 May 2019, revision 05 Nov 2019
Editor: Gareth Clay

Author for correspondence:
Sate Ahmad MSc., Department of Soil Physics, Faculty of Agricultural and Environmental Sciences, University of Rostock, Justus-von-Liebig-Weg 6,18059 Rostock, Germany
Tel: +49 (0) 381 498 3068; E-mail: sate.ahmad@uni-rostock.de

Appendix

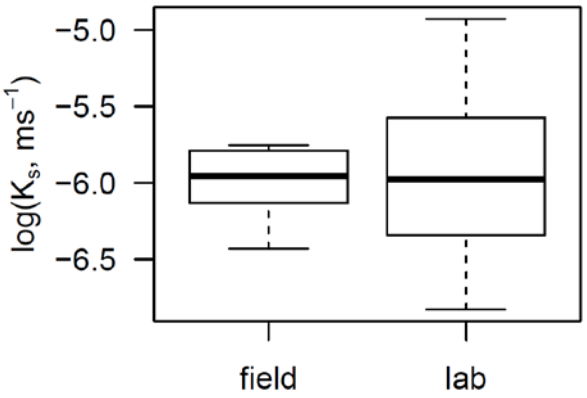

Figure A1: Comparison of K_s log-transformed values between field measurements using direct-push piezometer and laboratory measurements using constant-head upward-flow permeameter.

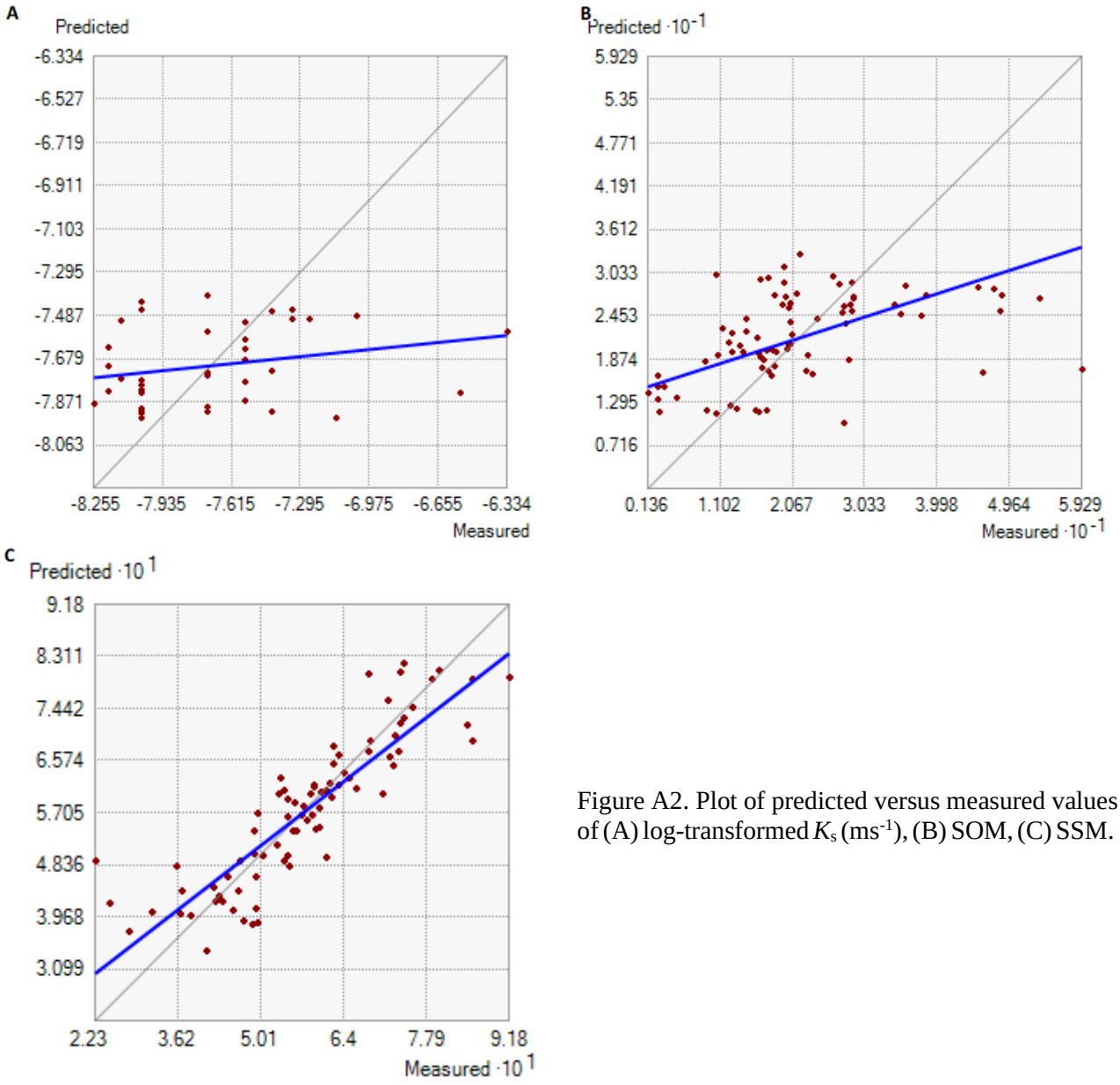

Figure A2. Plot of predicted versus measured values of (A) log-transformed K_s (ms^{-1}), (B) SOM, (C) SSM.

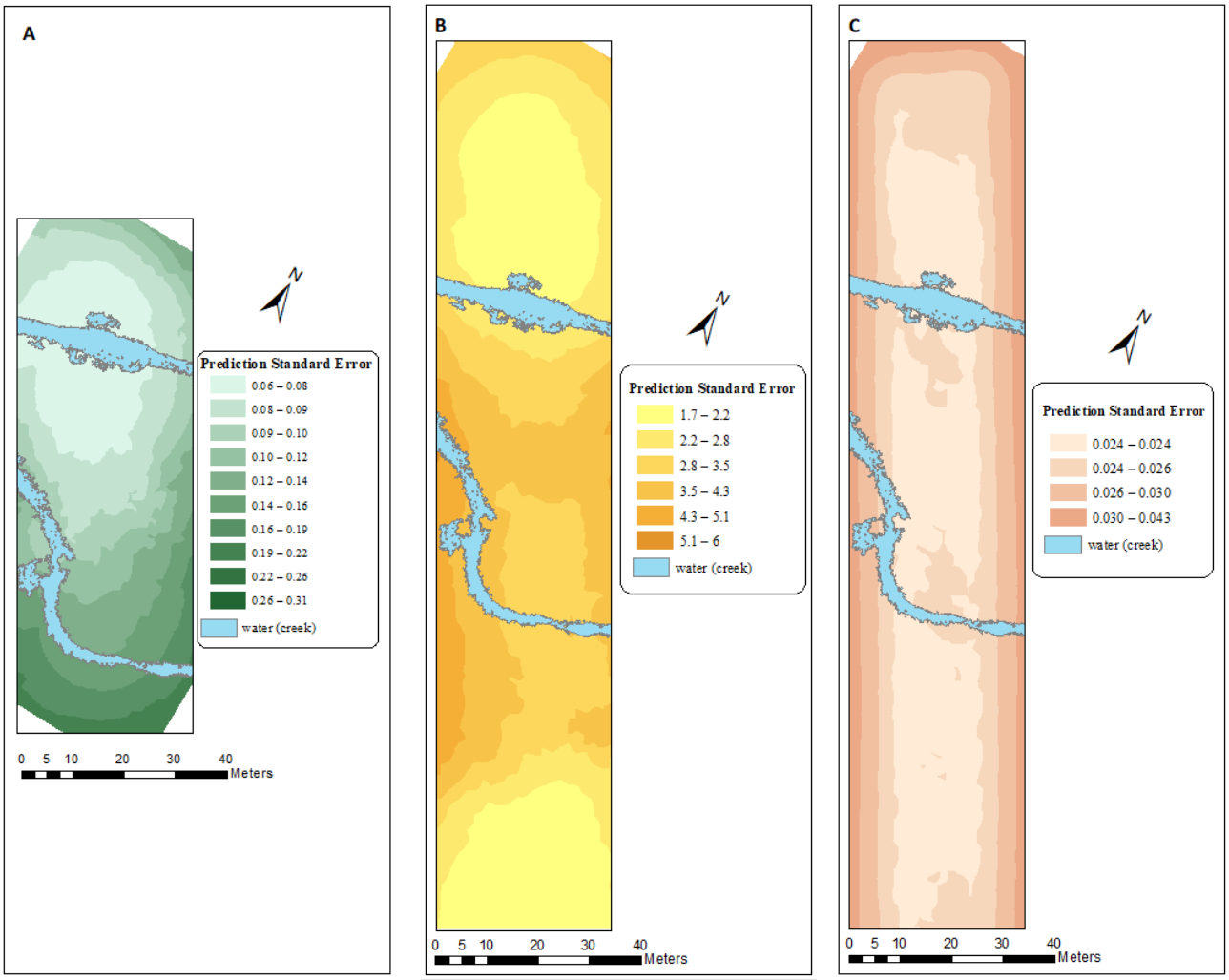

Figure A3. Contour map of Prediction Standard Error of (A) K_s, log-transformed (m s^{-1}), (B) SOM (%w/w), (C) SSM (in metres above mean sea level).